Artificial intelligence-enabled electrocardiogram to distinguish atrioventricular re-entrant tachycardia from atrioventricular nodal re-entrant tachycardia

Supplementary material

Supplementary methods

ECG pre-processing

As AVNRT or AVRT should be almost identical on each beat, long recordings are therefore unlikely to be needed. A 5s segment duration was selected as these performed better than 10s recordings on preliminary analyses. This is may be because twice as many 5s recordings are available for training from the same length recording compared to if 10s input recordings are used. Subsampling the ECG recording is an established methodology to reduce the number of model parameters ((1)) and can be seen as a form of data augmentation to allow the network to learn from the subtle variations in each sub sample. Given the current classification task was to diagnose arrhythmia mechanisms, ECG durations shorter than 5s were considered to be too short and therefore were not examined. A detailed comparison of ideal subsampling durations is beyond the scope of this manuscript.

Digital 12-lead ECGs were recorded using the EP recording system (LABSYSTEM™ PRO (Boston Scientific)) as previously described (2). ECGs were downsampled to 200hz as this was the lowest input sampling rate on validation data showed no differences in model accuracy, therefore 200hz was chosen to reduce the data input size and number of model parameters, which consequently would reduce training time. Digital ECG recordings from outside the EP lab were not available, therefore we were unable to compare performance of the network with ECGs not recording the EP recording system, however other than the higher original sampling rate there is no major difference in how the ECG is recorded.

Although a 12 lead ECG uses data from only 8 independent leads, all 12 leads were used as input in our neural network. It is possible that the model training time could have been shorter when using 8 leads. Given the candidate CNN architectures all used a 12 lead input, we did not train a model using 8 leads. It may also be possible to use a further limited number of leads (e.g. 1-4 leads from ambulatory monitoring) however this was not evaluated in the present study.

Architecture selection and hyperparameter optimization

1-dimensional convolutional neural network (CNN) architectures were implemented. The ECG signal is treated as a 1-dimensional time series with 12 channels. In order to fairly compare each candidate architecture, Keras tuner was used to perform a grid search to identify optimal hyperparameters for each architecture. Candidate architectures were: Zhu et al(3), Hannun et al(4), Attia et al (1), Ribeiro et al (5) Resnet 18, 34 and 50(6). Resnet 34 and Resnet 50 architectures did not generalise well during hyperparameter tuning, likely due to their large size, and therefore were excluded from further testing. Architectures were then compared to identify optimal performance as shown in supplementary table S1. Where architectures had similar performance, small networks with fewer parameters were preferred.

The final architecture was a modified version of that used by Attia et al (1). Their neural network architecture was used for a 2 second ECG segment, sampled at 500hz and zero padded to a final length of 1024. In contrast, given that our network is designed to make a rhythm diagnosis, we elected to use a longer ECG segment.

Our network therefore takes an input of a 5 second, sampled at 200hz and zero padded to a final length of 1024. During hyperparameter tuning, setting dropout to 0 resulted in the highest validation set accuracy. Therefore the dropout layer after the fully connected layer was removed, which was another difference to the network architecture of Attia et al. Lastly, the kernel size and number of filters for the last convolutional layer was not specified. A kernel size of 3 with 128 filters were chosen for the final convolutional layer in line with common convention of increasing the number of filters deeper into the network. Importantly, the final architecture was decided purely based on performance on the validation set.

Explainable artificial intelligence predictions

Saliency mapping has been used to explain CNN models ((2, 7, 8)). Grad-CAM is another method that has been used for this purpose (9). Grad-CAM identifies the last convolutional layer and investigates the gradients flowing into the layer. This works well for providing coarse localisation for images where a common kernel size is 5x5. This method however was not applicable to our model architecture given the small kernel size of 3 in the last convolutional layer. This kernel size results in the Grad-CAM mapping being far too coarse to be of any use. Other related methods such as guided Grad-CAM have been shown to be unreliable (10).

Test set

In order to directly compare model performance with the algorithm performance, one ECG per patient was used in the test as it would not be practical to manually evaluate a large number of ECGs using the manual algorithm. Additionally, each ECG segment is likely to be very similar to subsequent segments in the same patient, therefore the additive value of testing in all segments is likely to be negligible.

Supplementary figure S1
Flow chart of steps from patient population to prepared ECG inputs.

ECG: electrocardiogram; AVNRT: atrioventricular-nodal re-entrant tachycardia; AVRT: atrioventricular re-entrant tachycardia

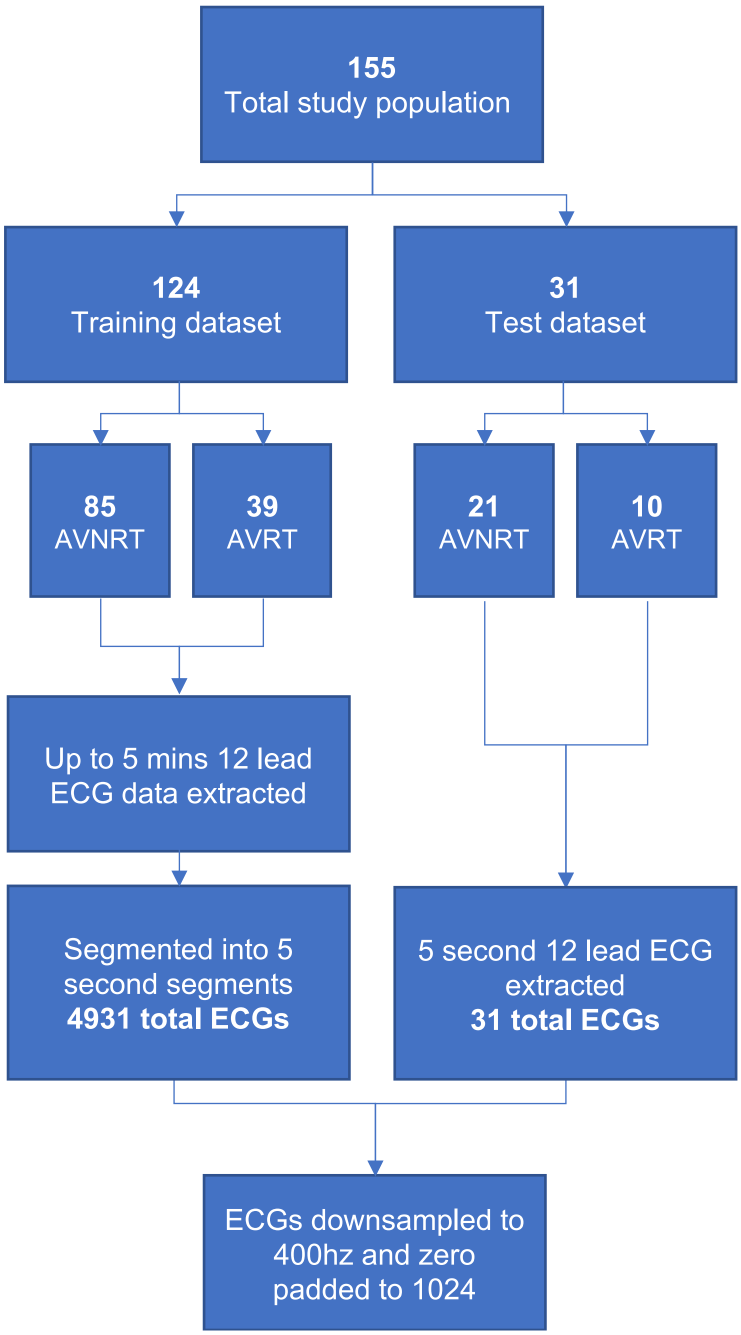

Supplementary figure S2

Flow chart of data flow from derivation of training dataset to model training. Testing dataset remains separate throughout and is used only for model evaluation

Supplementary figure S3

Selected model architecture is shown. Our final network was a modified version of one used by an Attia et al. (1). It is comprised of a total of 7 convolutional layers with 2 fully connected layers.

AVNRT: atrioventricular-nodal re-entrant tachycardia; AVRT: atrioventricular re-entrant tachycardia; Conv=convolutional layer; ReLU=rectified linear unit; F=number of filters; S=kernel size; MP=maxpool factor.

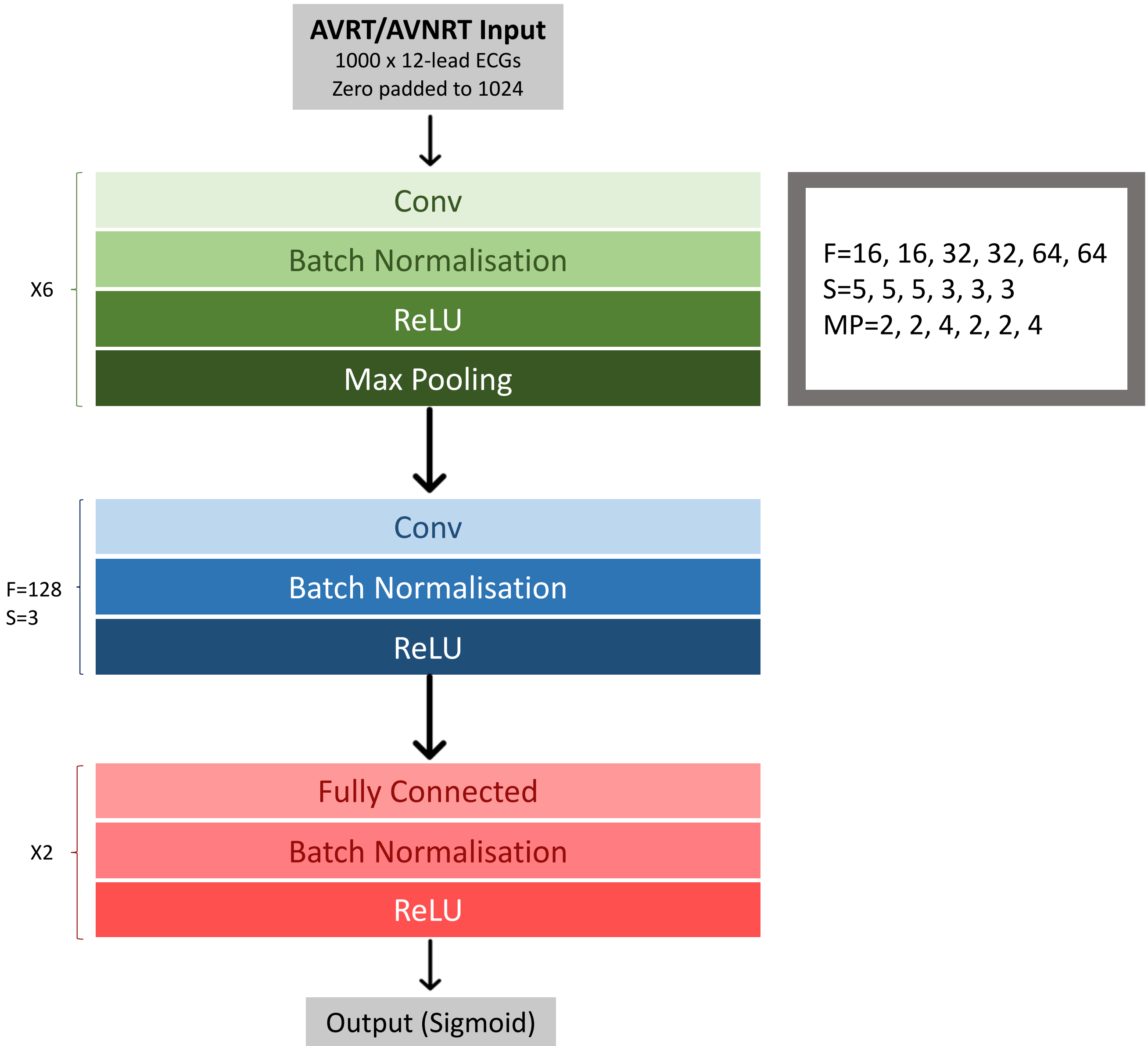

Supplementary figure S4

Algorithm schematic as described by Jaeggi et al. (11)

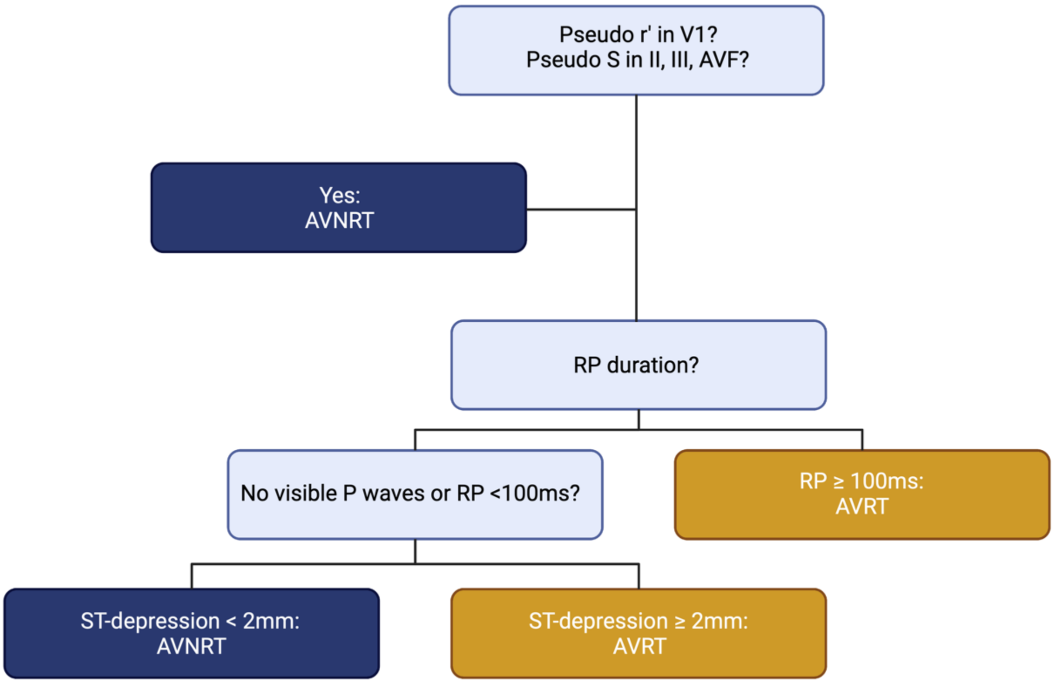

References

1. Attia ZI, Kapa S, Lopez-Jimenez F, McKie PM, Ladewig DJ, Satam G, et al. Screening for cardiac contractile dysfunction using an artificial intelligence-enabled electrocardiogram. Nat Med. 2019;25(1):70-4.
2. Arnold AD, Howard JP, Gopi A, Chan CP, Ali N, Keene D, et al. Discriminating electrocardiographic responses to His-bundle pacing using machine learning. Cardiovascular Digital Health Journal. 2020;1(1):11-20.
3. Zhu H, Cheng C, Yin H, Li X, Zuo P, Ding J, et al. Automatic multilabel electrocardiogram diagnosis of heart rhythm or conduction abnormalities with deep learning: a cohort study. The Lancet Digital Health. 2020;2(7):e348-e57.
4. Hannun AY, Rajpurkar P, Haghpanahi M, Tison GH, Bourn C, Turakhia MP, et al. Cardiologist-level arrhythmia detection and classification in ambulatory electrocardiograms using a deep neural network. Nat Med. 2019;25(1):65-9.
5. Ribeiro AH, Ribeiro MH, Paixao GMM, Oliveira DM, Gomes PR, Canazart JA, et al. Automatic diagnosis of the 12-lead ECG using a deep neural network. Nat Commun. 2020;11(1):1760.
6. He K, Zhang X, Ren S, Sun J, editors. Deep Residual Learning for Image Recognition. 2016 IEEE Conference on Computer Vision and Pattern Recognition (CVPR); 2016 27-30 June 2016.
7. Cohen-Shelly M, Attia ZI, Friedman PA, Ito S, Essayagh BA, Ko WY, et al. Electrocardiogram screening for aortic valve stenosis using artificial intelligence. Eur Heart J. 2021;42(30):2885-96.
8. Lima EM, Ribeiro AH, Paixao GMM, Ribeiro MH, Pinto-Filho MM, Gomes PR, et al. Deep neural network-estimated electrocardiographic age as a mortality predictor. Nat Commun. 2021;12(1):5117.
9. Selvaraju RR, Cogswell M, Das A, Vedantam R, Parikh D, Batra D. Grad-CAM: Visual Explanations from Deep Networks via Gradient-Based Localization. International Journal of Computer Vision. 2019;128(2):336-59.
10. Adebayo J, Gilmer J, Muelly M, Goodfellow I, Hardt M, Kim B. Sanity checks for saliency maps. Advances in neural information processing systems. 2018;31.
11. Jaeggi ET, Gilljam T, Bauersfeld U, Chiu C, Gow R. Electrocardiographic differentiation of typical atrioventricular node reentrant tachycardia from atrioventricular reciprocating tachycardia mediated by concealed accessory pathway in children. The American Journal of Cardiology. 2003;91(9):1084-9.